Depth of upper mantle seismic discontinuities.

B. TAUZIN[1], G.WITTLINGER[1], AND E.DEBAYLE[1]

[1]Institut de Physique du Globe, Strasbourg, FRANCE

E-mail: benoit.tauzin@eost.u-strasbg.fr

1 Introduction

The mantle transition zone, located in the depth range between 400 and 750 km, is a key-zone for understanding mantle dynamics. If in the last 10 years, seismic tomography has provided strong evidences for slab penetration in the lower mantle, observations of mantle upwelling from seismic tomography are still controversial. Additional constraints on mantle temperature and dynamics can be obtained from an improved imaging of discontinuity depths. Although P-to-S and S-to-P converted waves at the 410 and 660 km provide constraints for regions located below the earthquakes and receivers, the use of underside reflections from mantle discontinuities (SS precursors) is necessary to achieve a global coverage of the discontinuity topography. We aim to achieve a better mapping of the mantle transition zone by inverting simultaneously surface wave higher modes [1], SS precursors and converted waves for the 3D seismic structure and the depth variations of the 410 and 660 km discontinuities. Such a simultaneous inversion should allow us to minimize some of the trade-off present when higher modes and SS precursors/converted waves are interpreted separately. As a first step in this project, we have adaptated a receiver-function deconvolution technique to the processing of SS precursors. Our progress in the implementation of this approach as well as a first application to real SS precursor data are discussed in this poster.

2 Global coverage of the discontinuity topography

The SS-precursor data set

The SS seismic phase is the S wave underside reflection at the free surface of the Earth. All underside reflections of S waves on underneath interfaces, noted S_dS, arrive before the SS reference phase and are named consequently SS-precursors (Figures 1 and 2).

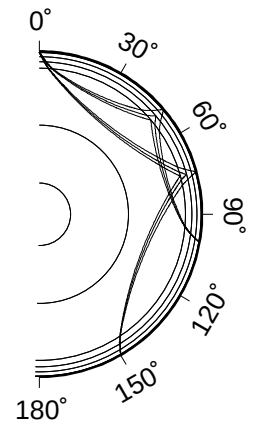

Figure 1. Paths of the SS reference phase and its precursors $S_{410}S$ and $S_{660}S$ in the IASP91 velocity model [2].

Assuming the velocity V_S in the upper layer is well -known, the time delay between the reference phase at a slowness p and its precursors gives the information of the depth h of the seismic discontinuity.

$$t_{SS} - t_{S_dS} \approx \frac{2h}{V_S}\sqrt{1 - p^2 V_S^2}$$

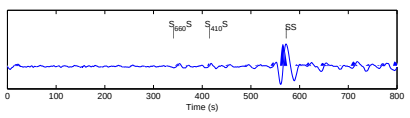

Figure 2. Seismogram at GDSN station OBN for an event at 131.7° range. Although, the two SS precursors ($S_{410}S$ and $S_{660}S$) are clearly visible, stacking techniques are usually necessary to separate them from the noise.

Halfway between the source and receiver, the bounce points of the SS precursors complement the informations provided by P-to-S and S-to-P receiver functions on the discontinuity depths beneath the stations.

3 Iterative deconvolution of SS-precursors

The amplitudes of SS precursors generally do not exceed 4-5 per cent of the SS reference phase amplitude so that SS precursors are difficult to separate from the noise. We adapt the well-known technique of receiver-function deconvolution to measure with precision the time delay between the SS-phase and its precursors.

3.1 Procedure

We assume a good resemblance between the SS reference waveform and its precursors and use the following procedure:

- We isolate the SS phase in a window on the transverse component of the record and use it as an SS reference waveform.
- At this stage we call the transverse component "signal" and use an iterative procedure that:
  1) performs a cross-correlation of the SS reference waveform and the signal.
  2) places a spike at the maximum of the resulting cross-correlogram.
  3) obtains a new "signal" by substracting the contribution of the SS reference waveform at the time pointed by the spike to the initial transverse component.
  4) come back to step 1.
  The iterative process is stopped when the effect of substrating the contribution of the SS reference at the time pointed by the spike is negligible.

Ideally, each spike should represent a (multiple) reflection on a discontinuity. The "SS receiver function" is obtained by convolving the succession of spikes in time with a gaussian (Figure 3).

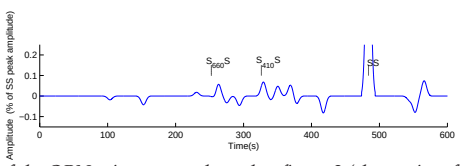

Figure 3. Iterative deconvolution of the OBN seismogram showed at figure 2 (the receiver function has been convolved with a gaussian function).

The deconvolution removes the source fonction on the transverse component of seismograms. Thus, stacking methods can be used to enhance the signal to noise ratio after aligning the SS reference peaks of each receiver function [3].

3.2 Synthetic tests for iterative deconvolution

In this section, we check on synthetics the effect of the data quality in the deconvolution and the influence of the number of data in post-deconvolution stacks. Our synthetic experiment follows several steps:

- We create a synthetic reference SS receiver function with one spike for the main SS phase and two spikes for the 410 and 660 precursors. The amplitude of the precursor spikes (black line on Figure 4b and 5) are 3% of the main SS spike.

Synthetic tests for iterative deconvolution (continued)

- We compute several hundred synthetic seismograms from the receiver function including realistic coloured noise (figure 4a).
- We apply iterative deconvolution on each synthetic seismogram and finally stack the resulting receiver functions.

1) We test several signal/noise ratio by imposing different noise levels (figure 4). The signal to noise ratio is computed by comparing the RMS energy amplitude in both the SS and its precursor windows. For this first test, we deconvolve 161 synthetic seismograms before stacking the resulting receiver functions.

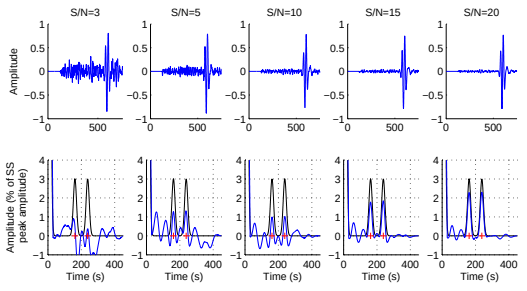

Figure 4. Effect of the signal/noise ratio on the deconvolution. The signal to noise ratio is indicated at the top of the plots.
a. Examples of synthetic seismograms with 3% SS-precursor amplitudes but varying noise levels. The noise spectrum is similar to the one observed at TAM station. For each signal/noise ratio value, we built 161 synthetic seimograms and obtain 161 receiver functions after deconvolution.
b. Final receiver functions (blue lines) obtained by stacking the resulting 161 receiver functions. The input (reference) receiver function is represented with the black lines in each plot and the red crosses indicate the SS-precursor peaks. For convenience, the receiver functions were returned so that SS reference peaks are at the left of each plot.

2) For a given signal to noise ratio ($S/N = 5$), we increase the number of seismograms in the stack (Figure 5). With higher signal to noise ratios ($S/N = 15$), a good recovery of the reference receiver function is obtained even with a smaller number of data (41 data).

Figure 5. Influence of the number of data in the stack. The number of data used in the stack is indicated at the top of the plots.
A signal/noise ratio of 5 is chosen for the tests.

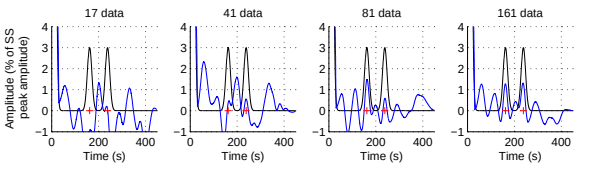

4 Preliminary results with real data

We processed 587 seismograms at the GEOSCOPE station TAM to study the impact of the signal to noise ratio and quantity of data on deconvolution and stack procedures. From the 587 initial seismograms, the number of data decreases with increasing signal to noise treshold values. This is illustrated on figure 6a where the first-order SS bounce points are represented. The post-deconvolution stacks for each data set of figure 6a are presented in figure 6b. We clearly see that the most influent parameter that controls the detection of the 410 and 660 km discontinuities is the number of data.

Figure 6. Application of the procedure on real seismograms at GEOSCOPE station TAM.

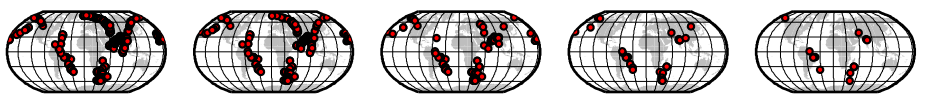

587 data - $S/N > 0$ 262 data - $S/N \geq 3$ 110 data - $S/N \geq 5$ 34 data - $S/N \geq 8$ 16 data - $S/N \geq 10$

a. SS bounce points (red points) location. From left to right, we increase the signal/noise ratio so decrease the number of data in the stack.

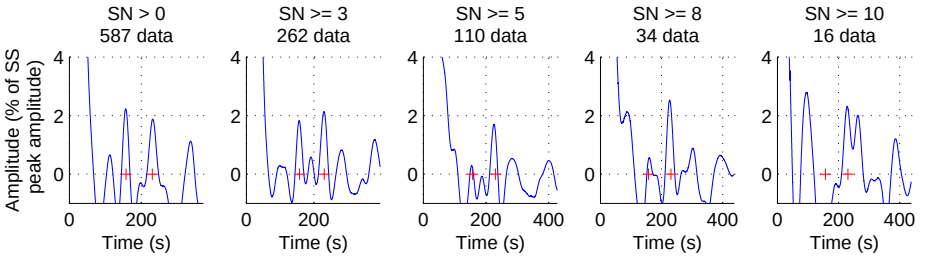

b. Result of the post-deconvolution stacks for the different signal/noise ratios. Red crosses indicate the expected location of the 410 and 660 km discontinuities.

5 Conclusions

On actual seismograms, the number of data involved in the stacks seems to be the most influential factor that controls the recovery of the SS precursors. On synthetics, the observation that an excellent recovery of the input receiver function can be achieved by increasing the signal to noise ratio (Figure 4) gives us confidence in the robustness of our deconvolution code and stacking approach. However, we have observed that increasing the number of data in the synthetic stacks does not always improve the recovery of the input receiver function. This may come from the characteristics of the input noise introduced in the synthetics. We are still working to understand what's going on in order to tune properly the different parameters controling the selection of data, deconvolution and stack. We will then be able to apply our deconvolution approach to a global dataset of SS precursors.

References

[1] E. Debayle, B. Kennett and K. Priestley (2005), Global azimuthal seismic anisotropy and the unique plate-motion deformation of Australia, *Nature*, **433**, 509-512.

[2] B. L. N. Kennett and E. R. Engdahl (1991), Traveltimes for global earthquake location and phase identification, *Geophys. J. Int.*,**105**, 429-465.

[3] M. P. Flanagan and P. M. Shearer (1998), Global mapping of topography on transition zone velocity discontinuities by stacking SS-precursors, *J. Geophys. Res.*, **103**, 2673-2692.